Received: 8 May 2018 | Revised: 10 July 2018 | Accepted: 8 August 2018

DOI: 10.1111/gcbb.12552

ORIGINAL RESEARCH

WILEY GLOBAL CHANGE BIOLOGY BIOENERGY

X-ray computed tomography to predict soil N_2O production via bacterial denitrification and N_2O emission in contrasting bioenergy cropping systems

Alexandra N. Kravchenko[1,2] | Andrey K. Guber[1] | Michelle Y. Quigley[1] | John Koestel[3] | Hasand Gandhi[4] | Nathaniel E. Ostrom[2,4]

[1]Department of Soil, Plant and Microbial Sciences, Michigan State University, East Lansing, Michigan

[2]DOE Great Lakes Bioenergy Research Center, Michigan State University, East Lansing, Michigan

[3]Swedish University of Agricultural Sciences, Uppsala, Sweden

[4]Department of Integrative Biology, Michigan State University, East Lansing, Michigan

Correspondence
Alexandra N. Kravchenko, Department of Soil, Plant and Microbial Sciences, Michigan State University, East Lansing, MI.
Email: kravche1@msu.edu

Funding information
DOE, Grant/Award Number: DE-SC0018409; National Science Foundation, Grant/Award Number: , 2017, 57314018; German Academic Exchange Service; Alexander von Humboldt Foundation

Abstract

While renewable biofuels can reduce negative effects of fossil fuel energy consumption, the magnitude of their benefits depends on the magnitude of N_2O emissions. High variability of N_2O emissions overpowers efforts to curb uncertainties in estimating N_2O fluxes from biofuel systems. In this study, we explored (a) N_2O production via bacterial denitrification and (b) N_2O emissions from soils under several contrasting bioenergy cropping systems, with specific focus on explaining N_2O variations by accounting for soil pore characteristics. Intact soil samples were collected after 9 years of implementing five biofuel systems: continuous corn with and without winter cover crop, monoculture switchgrass, poplars, and early-successional vegetation. After incubation, N_2O emissions were measured and bacterial denitrification was determined based on the site-preference method. Soil pore characteristics were quantified using X-ray computed microtomography. Three bioenergy systems with low plant diversity, that is, corn and switchgrass systems, had low porosities, low organic carbon contents, and large volumes of poorly aerated soil. In these systems, greater volumes of poorly aerated soil were associated with greater bacterial denitrification, which in turn was associated with greater N_2O emissions ($R^2 = 0.52$, $p < 0.05$). However, the two systems with high plant diversity, that is, poplars and early-successional vegetation, over the 9 years of implementation had developed higher porosities and organic carbon contents. In these systems, volumes of poorly aerated soil were positively associated with N_2O emissions without a concomitant increase in bacterial denitrification. Our results suggest that changes in soil pore architecture generated by long-term implementation of contrasting bioenergy systems may affect the pathways of N_2O production, thus, change associations between N_2O emissions and other soil properties. Plant diversity appears as one of the factors determining which microscale soil characteristics will influence the amounts of N_2O emitted into the atmosphere and, thus, which can be used as effective empirical predictors.

KEYWORDS
bacterial denitrification, computed microtomography, particulate organic matter, plant diversity, site-preference analysis, soil pore size distributions

1 | INTRODUCTION

Renewable biofuels provide a unique opportunity for reducing the negative effects of fossil fuel energy consumption (Qin, Zhuang, & Zhu, 2015). However, the benefits of biofuel cropping systems may be offset by their contribution to greenhouse gas emissions, in particular, N_2O (Johnson & Barbour, 2016; Oates et al., 2016; Qin et al., 2015; Walter, Don, & Flessa, 2015; Wightman, Duxbury, & Woodbury, 2015). Despite major efforts by scientific community to curb uncertainties in estimations of N_2O fluxes (Paustian et al., 2016; Robertson, Paul, & Harwood, 2000; van Groenigen, Osenberg, & Hungate, 2011), accurate predictions of soil N_2O emissions remain unattainable (Groffman et al., 2009; Harrison-Kirk, Beare, Meenken, & Condron, 2013; Henault, Grossel, Mary, Roussel, & Leonard, 2012; Huang, Grace, Mengersen, & Weier, 2011), which negatively affects the accuracy in estimating the benefits of biofuel systems. Even though the main processes behind soil N_2O production and emission are well understood (Butterbach-Bahl, Baggs, Dannenmann, Kiese, & Zechmeister-Boltenstern, 2013), the enormous microscale variability of the soil characteristics that influence these processes overpowers prediction efforts.

The majority of N_2O production in soils is driven by biologically mediated nitrogen transformations, among which, nitrification and denitrification are generally regarded as the most influential processes in majority of terrestrial ecosystems (Barnard, Leadley, & Hungate, 2005; Fowler et al., 2009). Out of the two, denitrification is frequently found to be highly spatially variable and more difficult to predict, while often the dominant source of soil N_2O production (Li, Sorensen, Olesen, & Petersen, 2016; Ostrom et al., 2010; Robertson & Tiedje, 1987). Oxygen deficiency is a necessary condition for denitrification to occur, and soil water-filled pore space (WFPS) levels in a 70%–80% range are regarded as optimal for denitrification (Butterbach-Bahl et al., 2013). Due to soil heterogeneity, anoxic conditions suitable for denitrification can occur in isolated microsites even within a well-aerated soil (Keiluweit, Gee, Denney, & Fendorf, 2018; Keiluweit, Nico, Kleber, & Fendorf, 2016; Keiluweit, Wanzek, Kleber, Nico, & Fendorf, 2017; Kravchenko et al., 2017; Loecke & Robertson, 2009; Sexstone, Revsbech, Parkin, & Tiedje, 1985). The size of such local anoxic spots can increase or decrease in response to not only physical drivers, that is, O_2 inflow from the atmosphere, but also biological activities of soil microorganisms consuming O_2. Emission of N_2O out of the soil also depends on the severity of O_2 depletion, which can facilitate N_2O reduction to N_2, and on the presence of N_2O escape routes, both governed by gas diffusion (Balaine et al., 2013; Ball, 2013; Mutegi, Munkholm, Petersen, Hansen, & Petersen, 2010). Further complicating matters are patterns of soil wetting/drying, resulting in differences in water distributions in the pore space for the same water contents, thus affecting gas diffusion rates in different parts of pore space and causing trapping of N_2O in air-disconnected pores (Guo, Drury, Yang, Reynolds, & Fan, 2014; Rabot, Henault, & Cousin, 2014, 2016). Yet another complication is added by influences on N_2O production from highly spatially variable N and C sources, such as decomposing plant residues (Kravchenko et al., 2017; Parkin, 1987).

N_2O production in soils is a consequence of the activity of nitrifying and denitrifying microorganisms and potentially abiotic processes. Definitive resolution of production pathways remains challenging; however, isotopic site-preference (S_P) analysis can provide considerable insight. S_P is defined as the difference in $\delta^{15}N$ between the central and outer N atoms in N_2O and has been shown to be constant during microbial production even though $\delta^{15}N$ and $\delta^{18}O$ vary or isotopically fractionate (Frame & Casciotti, 2010; Haslun, Ostrom, Hegg, & Ostrom, 2018; Sutka et al., 2006). Specifically, pure culture studies demonstrate that S_P values of 33‰–37‰ and −10 to 0‰, respectively, can be used to indicate N_2O production from hydroxylamine oxidation/fungal denitrification and bacterial denitrification (Sutka et al., 2006; Sutka, Ostrom, Ostrom, Gandhi, & Breznak, 2004). Based on these values, the proportion of N_2O derived from bacterial denitrification can be determined from the S_P value of soil-derived N_2O (Ostrom & Ostrom, 2011). Reduction of N_2O during denitrification has the potential to alter S_P; however, the magnitude of this effect is small (Jinuntuya-Nortman, Sutka, Ostrom, Gandhi, & Ostrom, 2008; Ostrom et al., 2007). Opdyke, Ostrom, and Ostrom, (2009 estimated that if 10% of produced N_2O was reduced, the shift in S_P would only be 0.7‰ and, further, would result in an underestimate of the importance of production from bacterial denitrification. The potential for abiotic production of N_2O in soils is increasingly being recognized and may be particularly important in Fe-rich soils and in the presence of nitrite (Zhu-Barker, Cavazos, Ostrom, Horwath, & Glass, 2015). Although potentially

variable (Buchwald, Grabb, Hansel, & Wankel, 2016), the S_P of N_2O produced by abiotic processes is generally in the range of 26‰–35 ‰ (Grabb, Buchwald, Hansel, & Wankel, 2017; Heil et al., 2014; Heil, Liu, Vereecken, & Bruggemann, 2015) and thus similar to the range expected for production via hydroxylamine oxidation and fungal denitrification. Bacterial denitrification largely stands alone with S_P values primarily in the range of 0‰–10‰ which provides a basis to constrain this process relative to other production pathways (Ostrom & Ostrom, 2011).

Most physical and biological processes that contribute to N_2O emissions vary in soil at scales of microns to millimeters (Kravchenko, Negassa, Guber, & Rivers, 2015; Nunan, Wu, Young, Crawford, & Ritz, 2003), and their variations may not always be well captured by bulk soil characteristics, for example, soil water content, measured on decimeter-scale soil samples (Ball, 2013). Size distribution, connectivity, tortuosity, and saturation of soil pores govern air and water fluxes in soil and, thus, influence N_2O production and N_2O emission from soil at microscales (Ball, 2013; Schurgers, Dorsch, Bakken, Leffelaar, & Haugen, 2006). However, these microscale characteristics are extremely difficult to quantify. One way to do this is by using X-ray computed microtomography (μCT) that enables visualization of soil pore geometry (Vogel, Weller, & Schluter, 2010; Wang, Kravchenko, Smucker, Liang, & Rivers, 2012). Moreover, it enables detection of plant roots and large fragments of organic material, that is, particulate organic matter (POM) (Kravchenko, Negassa, Guber, & Schmidt, 2014; Mooney & Morris, 2008). X-ray μCT images of intact soil samples allow analysis of these properties in situ and quantification of their influence on N_2O emissions (Mangalassery et al., 2014; Mangalassery, Sjogersten, Sparkes, Sturrock, & Mooney, 2013; Porre, Groenigen, Deyn, Goede, & Lubbers, 2016; Rabot, Lacoste, Henault, & Cousin, 2015).

The goal of this study was to assess the contribution of soil pore characteristics and POM to N_2O production via bacterial denitrification and to N_2O emissions from soils under several contrasting bioenergy cropping systems. We measured pore characteristics by μCT scanning and production of N_2O from bacterial denitrification using S_P analysis. The studied systems are continuous corn with and without winter cover crop, monoculture switchgrass, poplars, and early-successional vegetation. We hypothesize that long-term growth (9 years) of different plant species affects soil C and N levels as well as the presence, connectivity, and size distributions of soil pores. These characteristics, in turn, will influence C and N availability to microorganisms and will govern the ability of soil to retain water and to enable gas exchange, and thus will both directly and indirectly affect the N_2O production from denitrification and the emissions of N_2O overall.

Our first objective was to study presence, connectivity, and size distribution of soil pores with radii >30 μm, under the assumption that their absence leads to anoxic conditions, while presence contributes to O_2 and N_2O in- and outflows. The second objective was to explore the role of POM on N_2O production and emission. We hypothesized that greater presence of POM surrounded by soil with prevalence of large pores will lead to greater N_2O emissions. POM is a source of C and N, and its active decomposition can lead to local anaerobic conditions—both factors favoring N_2O production—while the presence of large pores in its vicinity would enhance air diffusion and therefore cause larger emissions of produced N_2O.

In addition, we explored the role of water distribution patterns in N_2O production and emission. Soil moisture and matric potential are the characteristics that define which soil pores and to which extent are filled with water. Due to the hysteresis of soil water retention, to which extent soil pores are filled with water at any moisture content and matric potential level depends on the history of soil wetting/drying. Generally, at the same matric potential, soil water content is higher, when an initially saturated soil is drained, as compared with a dry soil after rewetting. Because of hysteresis in soil water retention, the spatial distributions of water within the pore space vary. On the one hand, drying of the wet soil forms pockets of trapped water, which reduces gas diffusion and enhances local anoxic conditions. On the other hand, rewetting of dry soil results in trapping air in dead-end pores, which also affects the gas diffusion and local anoxic conditions in soils. To which extent the hysteresis of soil water retention affects N_2O production and N_2O emissions from soil is still unknown. We hypothesized that even though soil subjected to the wetting-up mode will have the same soil moisture or the same matric potential level as the soil subjected to the drying-down mode, it will still have lower N_2O production via denitrification and lower N_2O emissions.

2 | MATERIALS AND METHODS

2.1 | Experimental site and studied bioenergy systems

The experimental site is Great Lakes Bioenergy Center's Biofuel Cropping System Experiment located at Kellogg Biological Station, Michigan, USA, on well-drained Alfisol of Oshtemo and Kalamazoo series (mesic Typic Hapludalf; Robertson & Hamilton, 2015). The field experiment has been set up in 2008 as a randomized complete block design with five replications and with bioenergy systems assigned at random to 0.12 ha experimental plots within each replicated block. The five studied systems are two agronomic treatments: continuous corn (*Zea mays* L.) and continuous

corn with winter cover crop of cereal rye (*Secale cereale* L.), a monoculture switchgrass (*Panicum virgatum* L.), a hybrid poplar (*Populus nigra* × P. *maximowiczii* "NM6") with herbaceous understory (Sprunger & Robertson, 2018), and an early-successional community abandoned from agriculture in 2008. The experimental site was plowed prior to establishment, and no further plowing took place in any of the systems. The two continuous corn systems were managed as no-till. In the two corn systems, 168 kg N/ha of nitrogen fertilizer is applied annually, with 32 kg N/ha at planting and 136 kg N/ha as side-dress. Annually, 56 kg N/ha is applied to switchgrass and early-successional systems. The poplar system received a single application of 155 kg N/ha in 2010 and no annual applications of N. It should be noted that while, in general, these systems can be grown for several practical purposes, in this study, during the entire field experiment, all the systems were managed exclusively for bioenergy production. Thus, we refer to them as bioenergy systems. Detailed descriptions of the agronomic protocols, biomass harvest, and aboveground residue management are provided by Sanford et al. (2016) and Sprunger, Oates, Jackson, and Robertson (2017).

2.2 | Soil sampling

In this study, we collected soil samples only from four of the five replicated blocks of the field experiment. Intact soil cores (5 cm in diameter, 5 cm in height) were collected from four experimental plots of each cropping system, with 2–3 locations sampled within each plot, resulting in a total of 10 soil cores per cropping system. For each system, two cores were used for hysteresis measurements, and eight cores, that is, two cores from each experimental plot, were used in the incubation experiment. The cores were taken from depth of 5–10 cm in February of 2017, weighted, wrapped in an aluminum foil, and stored at 4°C.

2.3 | Water retention hysteresis

In order to determine hysteresis in soil of the studied treatments, water retention was measured using a modified evaporation method in two soil cores per cropping system (Wind, 1968). Round bottom ceramic cups (0.95 cm OD, 2.858 cm length, type 0652X07-B01M3, Soilmoisture Equipment Corp., Santa Barbara, CA) connected via pressure transducers (PX26-030DV, Omega Engineering, Inc., Stamford, CT) to a panel meter (DP25B, Omega Engineering, Inc., Stamford, CT) were installed into each core to record pressure head in the soil. Soil cores were, first, capillary saturated by keeping them for 48 hr on water-saturated coarse sand and then gradually fully saturated by increasing the water level around the cores. Saturated cores were weighed and subject to air-drying from the upper surface of the cores. The changes in the pressure head were recorded hourly. Once the change in the pressure head value approached 4–5 kPa, the cores were covered with a plastic cap to stop evaporation and kept for 24 hr to let water pressure equilibrate with the water content in the soil core. Then, soil cores were weighed, and the evaporation procedure was repeated. As a result, we obtained 15–20 approximately evenly spaced data points for the soil water retention curve. The measurements of the drainage curve of the water retention were stopped at pressure head $h = -70$ kPa.

The saturation limb of the soil water retention was measured in the same samples by incremental addition of water to the soil, followed by recording the pressure heads and weights of cores upon equilibrating pressure heads. The experiment was conducted until full soil saturation, that is, zero pressure head registered by the tensiometers. Then, soil water content was measured gravimetrically. The changes in the core weights were used for the soil moisture calculations at each pressure head.

2.4 | Incubation experiments

The remaining soil cores were split into three groups to study the effect of hysteresis in water retention on N_2O emission rates from the soil. The first group consisted of the cores that after full saturation were brought to −10 kPa pressure using a 5 bar pressure plate extractor (Soilmoisture Equipment Corp., Santa Barbara, CA) and are referred to as drying treatment (Dry). The second and third groups included soil cores that were, first, subject to drainage at −70 kPa and then rewetting, and are referred to as treatments rewetted to same pressure (WetPr) and to the same water content (WetWC). The WetPr treatment was rewetted to −10 kPa pressure head, while the WetWC treatment received water in the same amounts that were lost during the core drainage from −10 to −70 kPa. Therefore, presumably Dry and WetPr had the same pressure heads, but different water contents, while the Dry and WetWC treatments had similar water contents, but different pressure heads (Supporting information Figure S1). The number of replicated cores was 3 in the WetWC and Dry treatments and 2 in the WetPr treatment for each cropping system. Soil preparation for the incubation experiment was conducted in a cold room at 4°C to reduce the microbial activity and took from 7 to 10 days, depending on the time needed for saturation.

After soil cores were brought to their respective hysteresis conditions and weighed, a 1 cm layer was nondestructively cut from each core and used for water content determination. The cores were then placed into 16 oz Mason jars with two sealed rubber stoppers in the jar caps. A vial with 10 ml of water was placed into each jar to maintain high humidity in the jar and to prevent water evaporation from the soil. The seal in the lids was tested

using compressed air to prevent N_2O losses from the jars during incubation. N_2O content and S_P were measured after 72 hr incubation in the dark at temperature of 20°C, as described below. The soil samples were weighed to assure the absence of water content losses and then wrapped and stored in the cold room till X-ray μCT analysis.

2.5 | N_2O and S_P analysis

The relative importance of bacterial denitrification (including nitrifier denitrification) to total N_2O production was determined as described by Ostrom et al. (Ostrom et al., 2010). Specifically, pure culture studies demonstrate that S_P values of 33 to 37 and −10 to 0 ‰, respectively, indicate N_2O production from hydroxylamine oxidation + fungal denitrification and bacterial denitrification (Sutka et al., 2006). Based on these values, the proportion of N_2O derived from bacterial denitrification can be determined from the S_P value of soil-derived N_2O (Ostrom & Ostrom, 2011). We provide two estimates of the proportion of N_2O derived from bacterial denitrification: conservative and non-conservative based on endmember S_P values of −10‰ and 37‰ and 0‰ and 33‰, respectively (Kravchenko et al., 2017). The N_2O obtained from the soil cores was analyzed using a Trace Gas System (Elementar) interfaced to an Elementar Isoprime 100 mass spectrometer for determination of bulk $\delta^{15}N$, $\delta\ ^{18}O$, and S_P (Sutka et al., 2006). Within the Trace Gas System, water and CO_2 are removed using chemical scrubbers (magnesium perchlorate and Carbosorb, respectively), and N_2O is chromatographically separated from the residual CO_2 on a Porapak Q column that is interfaced to the mass spectrometer (Sutka et al., 2006). We applied corrections for the contribution of ^{17}O to masses 31 and 45 and for a small degree of rearrangement of ^{15}N between the α and β positions within the ion source (Toyoda & Yoshida, 1999). The concentration of N_2O is determined from the peak area of the *m/z* 44 trace during isotopic analysis with a reproducibility (1 *SD*) of 3% or better (Ostrom et al., 2010). The internal laboratory N_2O isotope standards were calibrated by analysis of USGS51 and USGS52 pure gas standards that have reported $\delta^{15}N$, $\delta^{18}O$, $\delta^{15}N^{\alpha}$, $\delta^{15}N^{\beta}$, and S_P values of 1.32, 41.23, 0.48, 2.15, and −1.67 and 0.44, 40.64, 13.52, −12.64, and 25.15‰, respectively (Ostrom et al., 2018).

2.6 | X-ray scanning

After incubation experiments, the cores were subjected to X-ray scanning using a GE Phoenix v|tome|x at the Institute of Soil and Environment at the Swedish University of Agricultural Sciences in Uppsala. The X-ray scanner was equipped with a 240 kV tube, a tungsten target, and a 16″ flat panel detector with 2,048 × 2,048 detector crystals (GE 1600). Each 3D X-ray μCT image was reconstructed from 2,000 projections acquired at a tube voltage of 130 kV and an electron flux of 200 μA. Each projection was obtained from the average of three consecutive radiographs recorded at the individual projection angles. The exposure time per radiograph was set to 200 ms. No optical filters were used during the image acquisition. 3D μCT X-ray images were reconstructed from the projections using the GE software datos|x. Each image had a resolution 29 μm in all directions.

2.7 | Image analysis

The X-ray μCT images were processed in ImageJ/Fiji software (Schindelin et al., 2012). A 2 voxel radius 3D median filter was applied to all images to remove random noise. A region of interest with a diameter and height of 4.5 cm was selected from the central portion of each μCT for the following analyses to avoid sampling artifacts close to the column walls.

For POM determination, we, first, visually identified a subset of 5–12 POM fragments from each core based on the grayscale value, size, and shape characteristics. The range of gray scale values was obtained from the central portion of each fragment. The average of the minimum and maximum gray scale values were then used as a threshold for initial POM identification. Then, a set of erosion/dilation steps was applied to eliminate boundary artefacts, followed by 3D Gaussian filter, and subsequent segmentation. Particle Analyser plugin (BoneJ) was then used to select only POM fragments with volume exceeding 0.016 mm^3.

Visible gravel/stone fragments >2 mm in size were delineated on the images using single threshold segmentation. Due to their higher attenuation coefficients, most stones are much brighter, that is, have higher grayscale values, than the other soil components, and thus are easy to segment. After thresholding, the >2 mm fraction was identified using Particle Analyser plugin with particle size >8 mm^3.

The X-ray resolvable soil pore network was obtained by first removing the areas delineated as POM and gravel from the X-ray images. The resulting images exhibited histograms in which gray scale values associated with air-filled pores were easily distinguished from ones pertaining to the soil matrix by using the minimum method. Pore size distributions with spatial locations of different pore radii were obtained using the maximal inscribable sphere method of Pore size distribution tool of Xlib plugin for ImageJ (Münch, 2008).

Given the scanning resolution of our μCT analysis, we could identify pores with radii >30 μm. In the subsequent description and discussion of the results, we interchangeably refer to such pores as either >30 μm pores or as visible pores.

To assess the size of the soil matrix that was not in close contact with >30 μm pores, we delineated a 180 μm wide zone around each μCT visible pore. It was assumed that due to proximity to large water-free pores, the soil within these zones has better aeration, than the remaining soil matrix. While choosing 180 μm for this delineation, we explored the patterns of changes in soil volume for a 30–810 μm range of distances from the pores (Supporting information Figure S1). The studied systems differed from each other the most in a 180–630 μm range, and 180 μm was consistent with spatial correlations reported for biological characteristics and soil C at microscales (Nunan et al., 2003; Quigley, Rivers, & Kravchenko, 2018); however, its choice is somewhat arbitrary in terms of gas diffusion. Delineation of 180 μm zone was conducted as a series of 3D dilations using 3D Dilate tool of ImageJ. The difference between the number of soil matrix voxels and the number of voxels belonging to the within the 180 μm zone was used in further data analyses as an indicator of the size of the volume of poorly aerated soil, and is referred to as Vol-180.

In order to assess POM's aeration status, we overlaid the 3D POM images with the images of μCT visible soil pores and identified the POM fragments that were or were not connected to the soil surface by the μCT visible pores. These two groups of POM fragments are referred to, respectively, as connected and unconnected POM.

2.8 | Statistical analysis

Comparisons among the bioenergy systems and hysteresis treatments in terms of the studied soil and N_2O measurements were conducted using a statistical model with the fixed effects of bioenergy system, hysteresis treatment, and their interaction and with the random effects of the two blocking factors involved in the experiment, that is, the experimental field blocks and the laboratory-processed blocks. Normality of the residuals and homogeneity of variances were checked for each studied variable. In case of marked deviations from normality, the data were log-transformed, for example, cumulative amount of emitted N_2O, while in case of variance heterogeneity, unequal variance analysis was performed (Milliken & Johnson, 2001). When inherent characteristics of the soil cores were correlated with N_2O measurements, for example, with WC during saturation, we conducted analysis of covariance (ANCOVA) and compared the effects of systems and hysteresis treatments after accounting for variations in these additional soil core characteristics (Milliken & Johnson, 2009). The analyses were conducted using PROC MIXED procedure of SAS (SAS Inc, 9.4).

Relationships among the studied continuous variables were first explored using correlation analyses conducted using the PROC CORR procedure of SAS and then were followed by fitting the relationships that were nonlinear with polynomial regression models using either PROC REG or PROC MIXED procedures. Comparisons among the studied systems in terms of parameters of the regression equations relating N_2O and soil variables, for example, regression slopes, were conducted using ANCOVA approach in PROC MIXED (Milliken & Johnson, 2009). Path analysis for examining influences on N_2O emissions was conducted as described in Wuensch (2016).

3 | RESULTS

3.1 | Soil characteristics

The soils of the studied bioenergy systems differed in a number of characteristics (Table 1). The two systems with high diversity of plant communities, that is, poplars and early-successional system, had significantly larger soil organic C and N contents than the two no-till corn-based systems. Poplar and early-successional systems had markedly higher total porosity and higher presence of visible pores. However, in terms of the presence of pores <30 μm the studied systems did not differ from each other.

The three systems with perennial vegetation, that is, switchgrass, poplars, and early-successional community, tended to have higher levels of POM than the annual corn systems, and continuous corn had significantly lower POM than the rest of the systems ($p < 0.1$). The volume of POM connected to the atmosphere by >30 μm pores in poplar and early-successional systems tended to be higher than that in corn with cover crops and switchgrass and exceeded that in the continuous corn.

The Vol-180, that is, the volume of poorly aerated soil, was the lowest in soils from poplar, followed by early-successional system, with the two not significantly different from each other, and was higher in the two corn systems and the switchgrass. At the time of field sampling, the systems did not differ in their water content levels, but the change in water content from the time of field sampling to the level at full saturation tended to be higher in poplars and early-successional systems. All systems had similar WFPS levels.

Soils from the two biodiverse systems, poplars and early succession, substantially differed from the other three systems in terms of their pore size distributions (Figure 1). These soils had higher abundance of 60–270 μm pores than the other three systems. The differences were particularly pronounced for pore sizes between 60 and 180 μm. The differences among corn and switchgrass systems in pore size distributions were not statistically significant, and even numerically the differences were very minor across the entire range of the studied pore sizes.

TABLE 1 Soil characteristics of the studied bioenergy systems. Shown are the means and the standard errors obtained in an ANOVA for each studied soil property along with p values from an F test for the bioenergy system effect ($n = 8$)

	Organic matter characteristics			
	SOC (g/kg)	**SON (g/kg)**	**Connected POM, % of total soil volume**	**Unconnected POM, % of total soil volume**
G1*	12.4a†	1.2a	0.36 b	0.17
G2	13.6a	1.4ab	0.70 ab	0.18
G5	14.5ab	1.3ab	0.78 ab	0.27
G8	16.8b	1.5bc	0.96 a	0.05
G9	17.9c	1.7c	1.12 a	0.15
Standard error	0.9	0.07	0.14	0.09
p value	0.01	0.05	0.1	NS
	Pore characteristics			
	Total porosity, %	Pores>30 μm, %	Pores <30 μm, %	Soil volume >180 μm away from >30 μm pores, %
G1	38.2 c	5.1 b	32.8	76.4 ab
G2	38.3 c	4.3 b	33.9	82.7 a
G5	37.2 c	5.3 b	32.1	76.3 ab
G8	48.4 a	11.0 a	37.3	65.0 b
G9	43.4 b	7.9 ab	35.6	72.3 ab
Standard error	1.6	1.4	2.0	4.8
p value	0.01	0.05	NS‡	0.1
	Soil moisture characteristics			
	Field water content (cm^3/cm^3)	Water-filled pore space before incubation (%)	Change in water content from field to saturation (cm^3/cm^3)	
G1	0.353	71.4	0.046 b	
G2	0.360	81.8	0.065 ab	
G5	0.363	81.2	0.058 ab	
G8	0.345	71.4	0.112 a	
G9	0.340	75.3	0.099 ab	
Standard error	0.026	3.8	0.018	
p value	NS	NS	0.05	

*G1: continuous corn; G2: continuous corn with cover crop; G5: switchgrass monoculture; G8: poplars; G9: early-successional vegetation. †Letters within each soil property identify systems significantly different from each other at the shown p value. ‡NS marks the cases when there were no significant differences among the studied systems.

3.2 | Isotopic composition of N_2O and percentage of N_2O derived from denitrification

The ranges in $\delta^{15}N$, $\delta^{18}O$, and SP for all samples analyzed are −33.2 to −0.4, 16.4 to 40.7, and −6.2 to 10.6 ‰ (Supporting information Table S1). These low SP values are consistent with a strong domination of N_2O production from bacterial denitrification (Ostrom & Ostrom, 2011). Based on these SP values, the proportion of N_2O derived from bacterial denitrification ranged from 55% to 91.9% or 64.3 to over 100% depending on whether the conservative or nonconservative model is used (Supporting information Table S1).

3.3 | Effect of bioenergy systems on N_2O

The bioenergy system effect on the proportion of N_2O generated via bacterial denitrification (N_2O-BD) was not statistically significant ($p = 0.11$). Numerically, corn with cover crop and early succession had lower N_2O-BD levels than

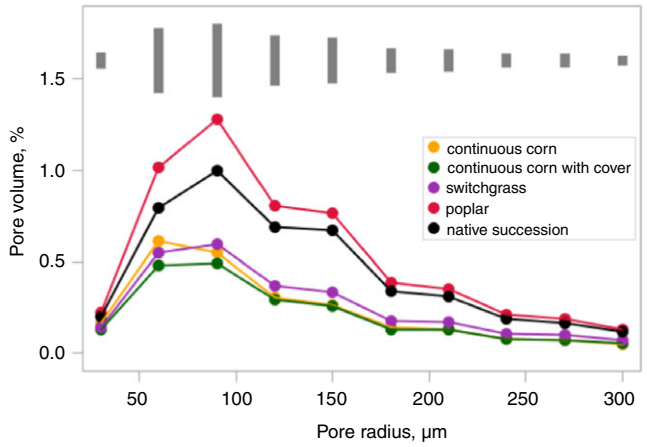

FIGURE 1 Pore size distribution for visible (>30 μm pores). Shown are the means and the values of least significant differences at $p < 0.05$ for each pore size class (gray bars; $n = 8$)

the other three systems (Figure 2a). Likewise, the bioenergy systems did not differ in the cumulative amount of N_2O emitted during 3 day incubations ($CumN_2O$). Numerically, the two biodiverse systems had somewhat lower $CumN_2O$ values than the low-diversity systems (Figure 2b), which is consistent with past field observations from this experimental site (Oates et al., 2016).

3.4 | Soil variables associated with proportion of N_2O generated via denitrification and with cumulative emitted N_2O

The five bioenergy systems separate into two distinct groups in terms of the relationships between soil characteristics and two N_2O variables, that is, N_2O-BD and $CumN_2O$. The first group consists of the two corn systems and switchgrass, which had lower soil C, low porosity, and low abundance of pores in 60–270 μm range. The second group consists of two biodiverse systems, poplars and early succession, which have high soil C levels, high porosity, and high abundances of pores in 60–270 μm range. Since the main management difference between these two groups is the diversity of their plant communities, we will refer to them as low-diversity and high-diversity systems, respectively.

In soils of low-diversity systems N_2O-BD was positively correlated with Vol-180 and negatively correlated with presence of pores in 30–120 μm size range (Table 2). The relationship between N_2O-BD and Vol-180 was nonlinear with quadratic regression explaining 22% of N_2O-BD variability (Figure 3a).

In soils of high-diversity systems, N_2O-BD was related to WFPS and, especially, to saturation of small pores (Table 2), however not to Vol-180 (Figure 3b). N_2O-BD in the high-diversity systems' soil was negatively related to the change in water content from field level to saturation (Table 2). Lower N_2O-BD levels were observed in the soil cores where the change in water content was large, while higher N_2O-BD levels tended to be present in the cores where such change was small. To some extent, this trend was present in low-diversity systems as well, excluding continuous corn, the system where a very narrow and low range of water content change values was observed (Figure 4).

In low-diversity systems, the relationships of $CumN_2O$ with soil variables were very similar to those of N_2O-BD, and included positive correlation with Vol-180 and negative correlations with presence of pores in 30–60 μm size range (Table 2). In high-diversity systems, $CumN_2O$ was strongly associated with several soil variables, including some of the studied water content variables, Vol-180, and pores in the 30–150 μm size group. While in both low- and high-diversity systems, $CumN_2O$ was positively related

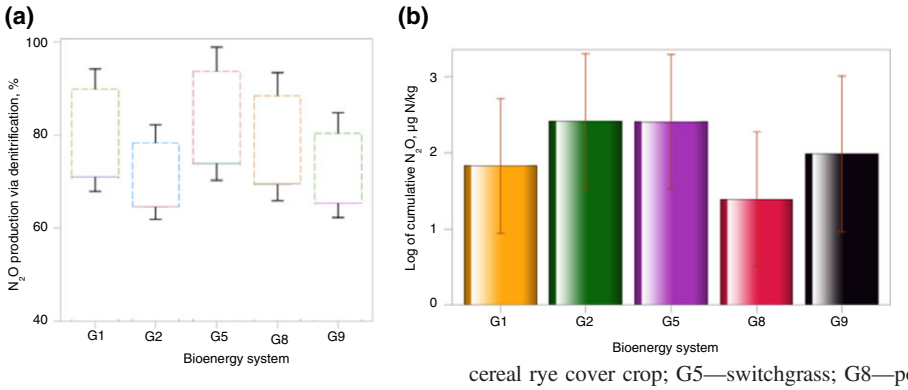

FIGURE 2 Proportion of N_2O generated via bacterial denitrification (a) and cumulative N_2O emitted during 3 day incubations per kg of stone free soil (b) from soil of the five studied bioenergy systems (G1—continuous corn; G2—continuous corn with cereal rye cover crop; G5—switchgrass; G8—poplar; G9—early-successional vegetation). The upper and lower boundaries of the boxes in (a) mark, respectively, the maximum and conservative estimates of the percentage of N_2O derived from denitrification. Shown are means and standard errors ($n = 8$)

TABLE 2 Correlation coefficients of proportion of N_2O generated via bacterial denitrification, N_2O-BD, and cumulative emitted N_2O, $CumN_2O$, with the selected soil characteristics

	Low diversity		High diversity	
	$CumN_2O$	N_2O-BD	$CumN_2O$	N_2O-BD
Water content (WC) variables				
WC before incubation	0.14	−0.11	**0.46**	0.37
WFPS	*0.36*	0.21	**0.65**	*0.50*
Total porosity	−0.10	−0.26	−0.20	−0.09
Change in WC from field to saturation	−0.26	−0.23	**−0.53**	**−0.60**
CT image-based variables				
Pores <30 μm	−0.14	−0.16	0.14	0.19
Pores >30 μm	0.07	−0.14	**−0.47**	−0.36
Saturation pores <30 μm	*0.33*	0.09	**0.66**	**0.52**
Saturation pores >30 μm	0.18	0.01	−0.07	*0.47*
Vol-180	*0.35*	**0.48**	**0.75**	0.09
POM total	−0.13	0.14	0.36	−0.03
POM connected by >30 μm pores	−0.02	0.11	0.21	−0.03
POM unconnected by >30 μm pores	−0.20	0.19	**0.68**	−0.03
Pores of average radius (μm)				
30	**−0.42**	**−0.48**	**−0.82**	0.16
60	**−0.39**	**−0.53**	**−0.77**	0.15
90	−0.27	**−0.48**	**−0.68**	0.12
120	−0.17	*−0.35*	**−0.57**	0.14
150	−0.11	−0.22	*−0.43*	0.08
180	−0.02	−0.14	−0.39	0.05

Notes. Correlation analysis was conducted separately in corn systems and switchgrass (low diversity) (n = ~24) and poplar and early-successional (high diversity) (n = ~16) systems. Correlation coefficients in bold and italic are significantly different from zero at $p < 0.05$ and $p < 0.1$, respectively

to Vol-180, WFPS, and saturation of small pores, the relationships were much stronger in high-diversity systems (Table 2, Figure 3).

Contrary to the expectations, neither the total POM nor connected or unconnected POM was related to N_2O-BD in either low- or high-diversity systems (Table 2). In low-diversity systems, $CumN_2O$ was not associated with either total POM or connected/unconnected POM. However, in high-diversity systems, the unconnected POM was strongly positively correlated with $CumN_2O$ (Figure 5).

The relationships between the two studied N_2O variables themselves, that is, N_2O-BD and $CumN_2O$, markedly differed between the low- and high-diversity systems (Figure 6). In low-diversity systems, the emitted $CumN_2O$ linearly increased as N_2O-BD increased from 60% to 80%, and slightly decreased as N_2O-BD increased to 90%. In high-diversity systems, $CumN_2O$ was not related to N_2O-BD at the range 60%–80%. Note that N_2O-BD values >80% were not observed in high-diversity systems.

3.5 | Effect of moisture regime

Numerically, the mean values of the N_2O-BD were the highest in Dry, followed by WetWC and WetPr water treatments, but the differences were not statistically significant (Figure 7a). The highest amount of N_2O was emitted from the Dry treatment (drying of wet soil), followed by WetWC (wetting dry soil to the same water content as Dry), and the lowest in WetPr (wetting dry soil to pressure similar to that of Dry, but higher than WetWC; Figure 7b).

4 | DISCUSSION

After 9 years of implementation, the bioenergy systems diverged into two distinct groups not only in terms of their organic matter and pore characteristics, but also in the factors contributing to N_2O production and emission. The latter is reflected by the differences between these two groups in terms of strengths and directions of the relationships between soil characteristics and N_2O variables. Specifically, in the low-diversity systems, corn and switchgrass, which had low C and low pore abundances, the emission of N_2O was strongly associated with the proportion of N_2O generated via bacterial denitrification. There both the proportion of N_2O generated via bacterial denitrification and the N_2O emission were greater at greater volumes of poorly aerated soil (Vol-180). However, water and pore characteristics explained only a small portion of variability in N_2O emissions in these systems. On the contrary, in the high-diversity systems, poplar and early succession, which had high C and high pore abundances, N_2O emission was not related to the proportion of N_2O generated via bacterial denitrification. Yet, a number of water and pore characteristics, notably Vol-180 and the abundance of unconnected POM, explained a substantial amount of variability in N_2O emissions in high-diversity systems.

Our data supported the hypothesis that long-term implementation of biofuel crops affects soil pore and water characteristics (Figure 1 and Table 1). Based on their pore characteristics, low- and high-diversity systems can be regarded, respectively, as those prone to high and low oxygen deficiency. Due to higher presence of >30 μm pores and lower Vol-180, the high-diversity systems had more favorable conditions for soil aeration and gas diffusion. On average, 88%–96% of POM in high-diversity systems was connected to the atmosphere by visible pores. On the contrary, the lower presence of >30 μm pores and higher Vol-

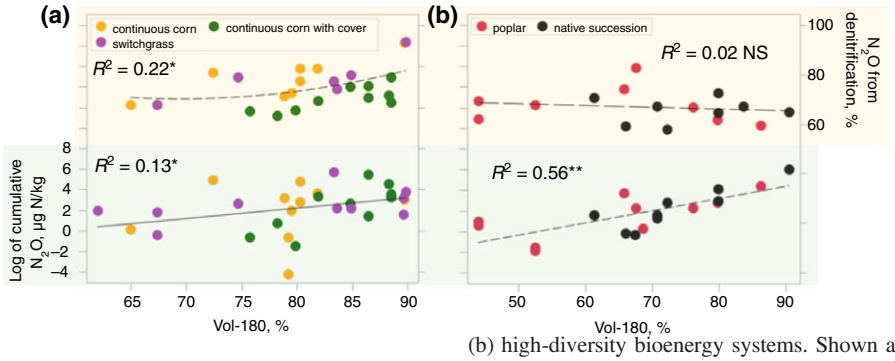

FIGURE 3 Relationship between the volume of poorly aerated soil, Vol-180, and N_2O derived from bacterial denitrification (conservative estimate) and total emitted N_2O in (a) low-diversity and (b) high-diversity bioenergy systems. Shown are individual data points and regression models, where ** and * mark the regression models statistically significant at $p < 0.05$ and $p < 0.1$, respectively

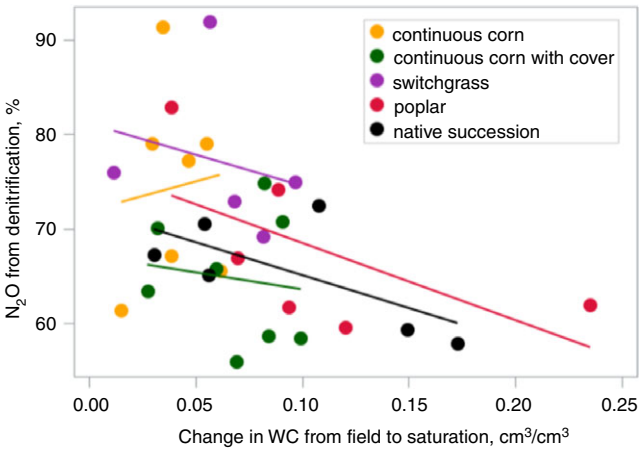

FIGURE 4 Association between the change in water content (WC) from field level to saturation and N_2O production via bacterial denitrification (conservative estimate) in the studied bioenergy systems

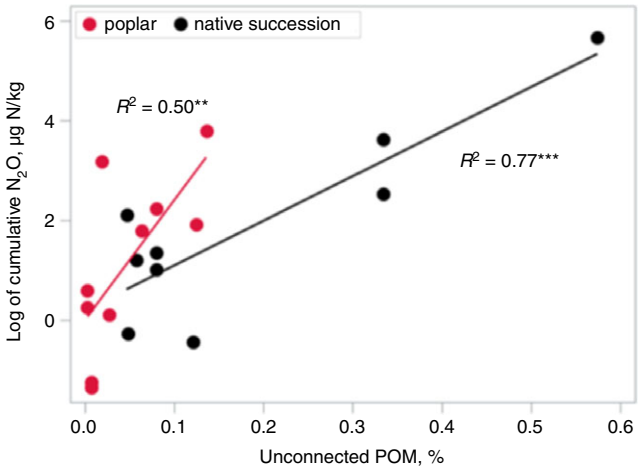

FIGURE 5 Associations between particulate organic matter (POM) unconnected to the soil surface by >30 µm pores and N_2O emissions in the bioenergy systems with high plant diversity. R^2 values marked with ** and *** are significant at the 0.05 and 0.01 levels, respectively

180 of the low-diversity systems suggest greater proneness to anoxic conditions. On average, only 70%–80% of POM in low-diversity systems was connected to the atmosphere by visible pores. Moreover, soil moisture conditions at the time of sampling demonstrated that indeed, low-diversity systems were less aerated, requiring smaller changes in water content at the time of sampling to reach full saturation (Table 1). This suggests that for a long time before the sampling, that is, during fall and winter months when evapotranspiration was low, the conditions within low-diversity systems could have been potentially more conducive to denitrification than in the high-diversity systems.

The results only partially supported the hypothesis regarding the importance of water retention hysteresis for N_2O emissions. It appeared that in this study, the actual water content, and not the mode in which it was reached, that is, wetting versus drying, mattered the most. The N_2O emissions from the soil that was dried and then brought to −10 kPa pressure were significantly lower than those from the soil that was dried to −10 kPa pressure after saturation as well as from the soil that, after drying, was wetted to the same water content.

We formulated a path model to relate aeration conditions, history of saturation, bacterial denitrification, and N_2O emissions and fitted it separately to data from low-diversity and from high-diversity systems (Figure 8). The model hypothesizes that the aeration conditions (represented by Vol-180) and a history of saturation (represented by the change in water content from field to saturation) influence N_2O-BD directly and influence CumN_2O both directly and indirectly through their effect on N_2O-BD.

4.1 | Soil characteristics related to proportion of N_2O produced via bacterial denitrification

The effect of anoxic conditions on N_2O-BD differed in low-diversity and high-diversity systems. In low-diversity

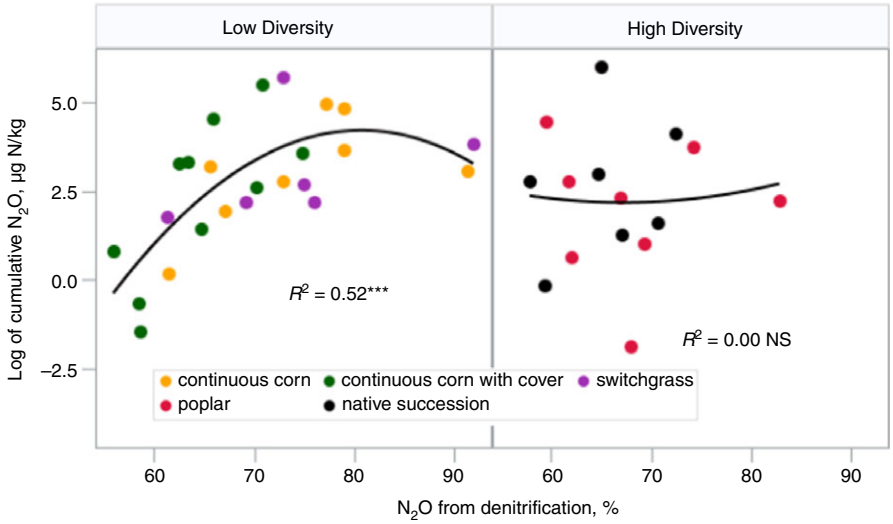

FIGURE 6 Associations between N_2O emission and percent of N_2O produced via bacterial denitrification (conservative estimate) in bioenergy systems with low and high plant diversity. R^2 values marked with *** and NS are significant at the $p < 0.01$ level and nonsignificant ($p > 0.1$), respectively

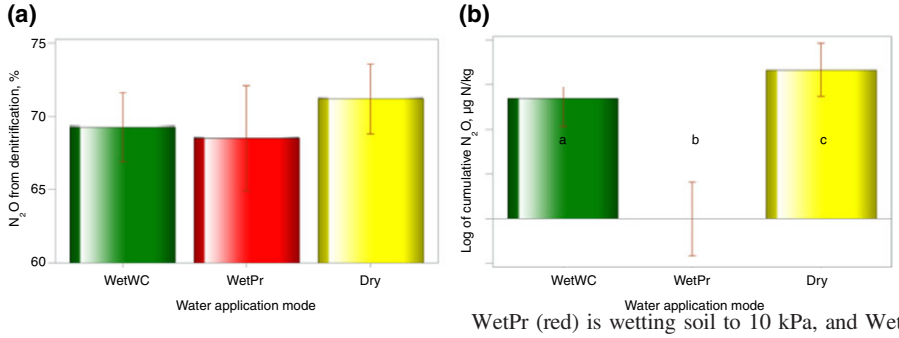

FIGURE 7 Proportion of N_2O generated via bacterial denitrification (conservative estimate) (a) and cumulative N_2O emitted during 3 day incubation (b) from soil of the three studied water application modes (Dry (yellow) is drying saturated soil to 10 kPa, WetPr (red) is wetting soil to 10 kPa, and WetWC (green) is wetting soil to the same water content initially present in Dry); shown are means adjusted for the change in the water contents during saturation values. Letters mark significant differences among water application modes ($p < 0.05$)

systems, lower aeration directly translated into lower N_2O-BD as indicated by (a) the negative relationship of N_2O-BD with abundance of 30–120 µm pores (Table 2), (b) the positive relationship of N_2O-BD with Vol-180 (Figure 3a, Table 2), and (c) the significant positive direct effect of Vol-180 on N_2O-BD (Figure 8). This result is consistent with dominance of bacterial denitrification in soil with higher water content and lower aeration reported by Well, Kurganova, Gerenyu, and Flessa (2006). Kravchenko et al. (2017) observed that in the absence of incorporated plant leaves, the proportion of N_2O from bacterial denitrification was higher in the soil with a prevalence of small (<10 µm) pores, the outcome driven by less aerated conditions in soils dominated by small pores and consistent with the results from low-diversity systems of this study. However, none of the indicators of low aeration associated with N_2O-BD in low-diversity systems were related to N_2O-BD in the high-diversity systems: There was no negative relationship of N_2O-BD with abundance of 30–120 µm pores (Table 2) and no positive relationship of N_2O-BD with Vol-180 (Figure 3b, Table 2). Moreover, Vol-180 had a significant negative direct effect on N_2O-BD in high-diversity systems (Figure 8).

Contrary to the expectations, the presence of POM was not related to N_2O-BD in either low- or high-diversity systems. Kravchenko et al. (2017) reported that when plant leaves were added to the soil, the proportion of N_2O generated via denitrification was higher in the soil with prevalence of large (>35 µm) pores than in the soil with prevalence of small (<10 µm) pores. They explained this result by formation of local anoxic conditions not within the soil, but within the decomposing leaves themselves. Hence, we hypothesized that in the soils of high-diversity systems, due to their higher amounts of POM and large pores, N_2O-BD also would be positively associated with POM and pore abundance. Yet, this hypothesis was not supported by the data and greater anoxic conditions, which could be surmised to occur within POM fragments due to enhanced decomposition (Kravchenko et al., 2017; Negassa et al., 2015), did not translate into greater N_2O production via bacterial denitrification.

The historic conditions in terms of water content levels preceding soil sampling appeared to be one of the few soil

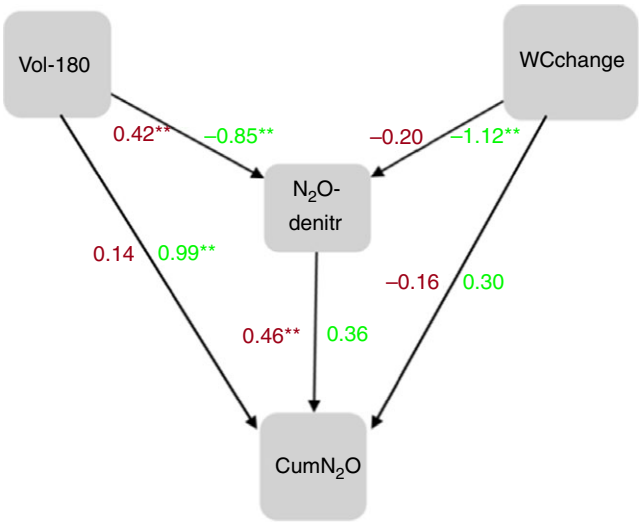

FIGURE 8 Path analysis model representing effects of the volume of poorly aerated soil, Vol-180, and historic absence of anoxic conditions (WCchange) on proportion of N_2O generated by bacterial denitrification (N_2O-BD) and on the total amount of emitted N_2O ($CumN_2O$). Coefficients in red are for low-diversity systems and in green are for high-diversity systems, and significant coefficients are marked by ** ($p < 0.05$)

characteristics significantly associated with N_2O-BD in high-diversity systems. In high-diversity systems, the change in the water content at the time of sampling needed to reach full saturation was negatively correlated with N_2O-BD (Table 2), and in the studied path model, it had statistically significant negative effect on N_2O-BD (Figure 8). Note that in the low-diversity systems, these associations also had a negative sign, but were not statistically significant. The closer the soil was to full saturation at the time of sampling, the greater the proportion of N_2O generated via bacterial denitrification. This relationship suggests that historic presence of denitrification-favorable conditions plays a positive role in current denitrification processes. It can be inferred that if the soil was held for a long period of time at conditions close to saturation, then denitrifying communities may have proliferated and expanded from small pores and aggregate centers, where they typically reside (Ebrahimi & Or, 2015; Tiedje, Sexstone, Parkin, Revsbech, & Shelton, 1984). Soil samples for this study were collected in February, after ~3 months of high soil moisture levels. Their denitrifying communities were not likely affected by sampling or sample preprocessing; thus, they continued to actively function during the incubation experiment of this study. The potential importance of adaptation history in defining the ability of microbial communities to produce N_2O has been expressed before (Jungkunst, Freibauer, Neufeldt, & Bareth, 2006; Krause et al., 2017; Lagomarsino et al., 2016), while the history of soil moisture conditions was found to play an unexpectedly greater role than current soil water levels for other soil processes, for example, soil respiration (Smith, 2017).

4.2 | Soil characteristics related to N_2O emission

Despite some similarities between low- and high-diversity systems in terms of associations between emitted N_2O and the soil aeration-related variables, overall, the two systems differed substantially, and the difference was most remarkable for $CumN_2O$ versus N_2O-BD relationship. In the low-diversity systems, greater proportion of N_2O from bacterial denitrification directly translated into greater N_2O emissions (Figure 6a, Figure 8). The magnitude of anoxic conditions, as indicated by (a) greater area of unaerated soil volume Vol-180 and (b) lower presence of 30–60 μm pores, appeared to be the main physical factor driving both the proportion of bacterial denitrification and N_2O emissions in these soils. In the high-diversity systems, bacterial denitrification had a statistically nonsignificant, but numerically also positive, direct effect on emitted N_2O (Figure 8). However, the straightforward pathway of poor aeration leading to greater contribution from bacterial denitrification to greater N_2O emissions, which was clearly observed in low-diversity systems, was not present in high-diversity soils.

In soils of high-diversity systems, poor aeration conditions led to substantially greater N_2O emissions directly. The positive effect of poor aeration was manifested through (a) negative relationship of $CumN_2O$ with presence of 30–120 μm pores (Table 2), (b) positive relationship of $CumN_2O$ with Vol-180 and with the POM unconnected to the atmosphere by visible pores (Figure 3b and Figure 5), and (c) positive relationship of $CumN_2O$ with WFPS and saturation of small pores (Table 2). Yet, while poor aeration did favor increased N_2O emissions, it did so without a concomitant increase in the proportion of N_2O produced via bacterial denitrification. In fact, the direct effect of Vol-180 on $CumN_2O$ (0.99) and its indirect effect on $CumN_2O$ via N_2O-BD mediation (−0.31) (calculated as a product of −0.85 and 0.46) had opposite signs. This inconsistency suggests that in these soils, other anaerobic processes besides bacterial denitrification contributed to N_2O production, perhaps fungal denitrification. The S_P of N_2O produced by fungi has been shown to be ~37‰ (Rohe et al., 2014; Sutka, Adams, Ostrom, & Ostrom, 2008), which is substantially greater than the values of −10 to 0‰ associated with production from bacterial denitrification (Frame & Casciotti, 2010; Sutka et al., 2006; Toyoda & Yoshida, 1999). Fungi have been demonstrated to denitrify at more oxic conditions than bacteria and to be a substantial contributor to N_2O production, especially in woody soils, but also in grasslands and soils of agricultural systems (Chen

& Shi, 2017; Chen, Mothapo, & Shi, 2014; Crenshaw, Lauber, Sinsabaugh, & Stavely, 2008; Laughlin & Stevens, 2002). Fungi were found to be in a greater abundance in poplar and early-successional, however also in switchgrass, systems of this study than in corn-based systems (Jesus et al., 2016). In soils of high-diversity systems, it is possible that fungal denitrification activity may be more responsive than bacterial denitrification to decreases in soil aeration, while in soils of low-diversity systems, an increase in fungal denitrification upon decreasing aeration was less noticeable, due, in part, to the lower abundance of fungi (Jesus et al., 2016). Note that denitrification by fungi only results in N_2O, but not N_2 production, since fungi lack the capability of N_2O to N_2 reduction (Prendergast-Miller, Baggs, & Johnson, 2011; Sutka et al., 2008). Since N_2O is the terminal product of denitrification by fungi, then fungal denitrification can be expected to result in more straightforward associations between N_2O emissions and the factors contributing to it, as the additional nonlinear effect of reduced N_2O production via its reduction to N_2 is eliminated. This could be a potential explanation for better predictive powers of soil water and pore characteristics observed in high-diversity systems of this study. It should be also noted that N_2O reduction to N_2 was more likely to take place in poorly aerated soils of low-diversity systems, and, due to tendency for fungi to live in larger pores with greater air diffusion, was likely more affecting N_2O of bacterial than fungal origin. This would explain lack of differences in the average values of $CumN_2O$ and N_2O-BD among the studied systems. Further assessment of fungal denitrification and fungal presence in these soils is needed to test this hypothesis.

It should be also noted that reduction of N_2O can alter SP; however, reduction shifts the relationship between $\delta^{18}O$ and $\delta^{15}N$ and $\delta^{18}O$ and $\delta^{15}N^{\alpha}$ shift toward 2.6 and 1.9, respectively, when reduction occurs (Ostrom et al., 2006; Jinuntuya-Nortman et al, 2008). Based on the data in Supporting information Table S1, we observed relationships between $\delta^{18}O$ and $\delta^{15}N$ and $\delta^{18}O$ and $\delta^{15}N^{\alpha}$ of 0.45 and 0.46, respectively, that are not consistent with a strong influence of N_2O reduction in our samples (Ostrom & Ostrom, 2011). Further, as discussed in the Introduction section, reduction of N_2O equal to 10% of its production will only shift S_P by 0.7 ‰ (Opdyke et al., 2009), which has a minor effect on our estimates of the importance of bacterial denitrification.

The findings indicated that several years of implementing bioenergy systems with contrasting plant diversities led to substantial changes in soil pore characteristics, along with soil C and N levels. These changes were likely one of the contributors to the observed differences in associations between N_2O emissions and soil microscale variables in bioenergy systems with low and high plant diversities. Contrary to the expectations, none of the studied pore or POM characteristics worked as an effective predictor of N_2O emissions across the entire set of the systems. However, saturation of <30 μm pores, presence of air-filled 30–90 μm pores, size of poorly aerated soil volume, and volume of POM unconnected to the atmosphere appeared to be feasible microscale soil predictors of N_2O emissions in soils from bioenergy systems with high plant diversity. Yet, in the systems with low plant diversity, N_2O production via bacterial denitrification appeared to be the only feasible predictor of N_2O emissions, while predictive capabilities of microscale pore and POM data were relatively weak. The possible cause is that long-term differences in implementing contrasting bioenergy systems may have affected the relative contributions of different processes, for example, bacterial and fungal denitrification and nitrification, to N_2O production and further reduction. Differences in influences from physical microscale soil characteristics on these processes likely led to the observed differences in capabilities of different soil characteristics in predicting N_2O emissions.

ACKNOWLEDGEMENTS

This work was funded in part by National Science Foundation's Long-Term Ecological Research Program (DEB 1027253) and by the National Science Foundation's Geobiology Program 460 (Award #1630399). This material is partly based upon work supported by the US Department of Energy, Office of Science, Office of Biological and Environmental Research, under Award Number DE-SC0018409, and work funded by the DOE Great Lakes Bioenergy Research Center (DOE BER Office of Science DE-FC02-07ER64494). The work of A. Kravchenko was supported by DAAD-German Academic Exchange Service's program "Research Stays for University Academics and Scientists, 2017" (57314018) and by the Research Award from the Alexander von Humboldt Foundation.

ORCID

Alexandra N. Kravchenko http://orcid.org/0000-0001-5920-927X

REFERENCES

Balaine, N., Clough, T. J., Beare, M. H., Thomas, S. M., Meenken, E. D., & Ross, J. G. (2013). Changes in relative gas diffusivity explain soil nitrous oxide flux dynamics. *Soil Science Society of America Journal*, *77*, 1496–1505. https://doi.org/10.2136/sssaj2013.04.0141

Ball, B. C. (2013). Soil structure and greenhouse gas emissions: A synthesis of 20 years of experimentation. *European Journal of Soil Science*, *64*, 357–373. https://doi.org/10.1111/ejss.12013

Barnard, R., Leadley, P. W., & Hungate, B. A. (2005) Global change, nitrification, and denitrification: A review. *Global Biogeochemical Cycles*, *19*. https://doi.org/10.1029/2004GB002282.

Buchwald, C., Grabb, K., Hansel, C. M., & Wankel, S. D. (2016). Constraining the role of iron in environmental nitrogen transformations: Dual stable isotope systematics of abiotic NO_2-reduction by Fe(II) and its production of N2O. *Geochimica Et Cosmochimica Acta*, *186*, 1–12. https://doi.org/10.1016/j.gca.2016.04.041

Butterbach-Bahl, K., Baggs, E. M., Dannenmann, M., Kiese, R., & Zechmeister-Boltenstern, S. (2013). Nitrous oxide emissions from soils: How well do we understand the processes and their controls? *Philosophical Transactions of the Royal Society of London. Series B, Biological Sciences*, *368*, 20130122.

Chen, H. H., Mothapo, N. V., & Shi, W. (2014). The significant contribution of fungi to soil N_2O production across diverse ecosystems. *Applied Soil Ecology*, *73*, 70–77. https://doi.org/10.1016/j.apsoil.2013.08.011

Chen, H. H., & Shi, W. (2017). Opening up the N_2O-producing fungal community in an agricultural soil with a cytochrome p450nor-based primer tool. *Applied Soil Ecology*, *119*, 392–395. https://doi.org/10.1016/j.apsoil.2017.07.022

Crenshaw, C. L., Lauber, C., Sinsabaugh, R. L., & Stavely, L. K. (2008). Fungal control of nitrous oxide production in semiarid grassland. *Biogeochemistry*, *87*, 17–27. https://doi.org/10.1007/s10533-007-9165-4

Ebrahimi, A., & Or, D. (2015). Hydration and diffusion processes shape microbial community organization and function in model soil aggregates. *Water Resources Research*, *51*, 9804–9827. https://doi.org/10.1002/2015WR017565

Fowler, D., Pilegaard, K., Sutton, M. A., Ambus, P., Raivonen, M., Duyzer, J., … Granier, C. (2009). Atmospheric composition change: Ecosystems-atmosphere interactions. *Atmospheric Environment*, *43*, 5193–5267. https://doi.org/10.1016/j.atmosenv.2009.07.068

Frame, C. H., & Casciotti, K. L. (2010). Biogeochemical controls and isotopic signatures of nitrous oxide production by a marine ammonia-oxidizing bacterium. *Biogeosciences*, *7*, 2695–2709. https://doi.org/10.5194/bg-7-2695-2010

Grabb, K. C., Buchwald, C., Hansel, C. M., & Wankel, S. D. (2017). A dual nitrite isotopic investigation of chemodenitrification by mineral-associated Fe(II) and its production of nitrous oxide. *Geochimica Et Cosmochimica Acta*, *196*, 388–402. https://doi.org/10.1016/j.gca.2016.10.026

Groffman, P. M., Butterbach-Bahl, K., Fulweiler, R. W., Gold, A. J., Morse, J. L., Stander, E. K., … Vidon, P. (2009). Challenges to incorporating spatially and temporally explicit phenomena (hotspots and hot moments) in denitrification models. *Biogeochemistry*, *93*, 49–77. https://doi.org/10.1007/s10533-008-9277-5

Guo, X. B., Drury, C. F., Yang, X. M., Reynolds, W. D., & Fan, R. Q. (2014). The extent of soil drying and rewetting affects nitrous oxide emissions, denitrification, and nitrogen mineralization. *Soil Science Society of America Journal*, *78*, 194–204. https://doi.org/10.2136/sssaj2013.06.0219

Harrison-Kirk, T., Beare, M. H., Meenken, E. D., & Condron, L. M. (2013). Soil organic matter and texture affect responses to dry/wet cycles: Effects on carbon dioxide and nitrous oxide emissions. *Soil Biology & Biochemistry*, *57*, 43–55. https://doi.org/10.1016/j.soilbio.2012.10.008

Haslun, J. A., Ostrom, N. E., Hegg, E. L., & Ostrom, P. H. (2018). Estimation of isotope variation of N_2O during denitrification by *Pseudomonas aureofaciens* and *Pseudomonas chlororaphis*: Implications for N_2O source apportionment. *Biogeosciences*, *15*, 3873–3882.

Heil, J., Liu, S. R., Vereecken, H., & Bruggemann, N. (2015). Abiotic nitrous oxide production from hydroxylamine in soils and their dependence on soil properties. *Soil Biology & Biochemistry*, *84*, 107–115. https://doi.org/10.1016/j.soilbio.2015.02.022

Heil, J., Wolf, B., Bruggemann, N., Emmenegger, L., Tuzson, B., Vereecken, H., & Mohn, J. (2014). Site-specific N-15 isotopic signatures of abiotically produced N_2O. *Geochimica Et Cosmochimica Acta*, *139*, 72–82.

Henault, C., Grossel, A., Mary, B., Roussel, M., & Leonard, J. (2012). Nitrous oxide emission by agricultural soils: A review of spatial and temporal variability for mitigation. *Pedosphere*, *22*, 426–433. https://doi.org/10.1016/S1002-0160(12)60029-0

Huang, X. D., Grace, P., Mengersen, K., & Weier, K. (2011). Spatio-temporal variation in soil derived nitrous oxide emissions under sugarcane. *Science of the Total Environment*, *409*, 4572–4578. https://doi.org/10.1016/j.scitotenv.2011.07.044

Jesus, E. D., Liang, C., Quensen, J. F., Susilawati, E., Jackson, R. D., Balser, T. C., & Tiedje, J. M. (2016). Influence of corn, switchgrass, and prairie cropping systems on soil microbial communities in the upper Midwest of the United States. *Global Change Biology Bioenergy*, *8*, 481–494. https://doi.org/10.1111/gcbb.12289

Jinuntuya-Nortman, M., Sutka, R. L., Ostrom, P. H., Gandhi, H., & Ostrom, N. E. (2008). Isotopologue fractionation during microbial reduction of N_2O within soil mesocosms as a function of water-filled pore space. *Soil Biology & Biochemistry*, *40*, 2273–2280. https://doi.org/10.1016/j.soilbio.2008.05.016

Johnson, J. M. F., & Barbour, N. W. (2016). Nitrous oxide emission and soil carbon sequestration from herbaceous perennial biofuel feedstocks. *Soil Science Society of America Journal*, *80*, 1057–1070. https://doi.org/10.2136/sssaj2015.12.0436

Jungkunst, H. F., Freibauer, A., Neufeldt, H., & Bareth, G. (2006). Nitrous oxide emissions from agricultural land use in Germany—A synthesis of available annual field data. *Journal of Plant Nutrition and Soil Science-Zeitschrift Fur Pflanzenernahrung Und Bodenkunde*, *169*, 341–351. https://doi.org/10.1002/jpln.200521954

Keiluweit, M., Gee, K., Denney, A., & Fendorf, S. (2018). Anoxic microsites in upland soils dominantly controlled by clay content. *Soil Biology & Biochemistry*, *118*, 42–50. https://doi.org/10.1016/j.soilbio.2017.12.002

Keiluweit, M., Nico, P. S., Kleber, M., & Fendorf, S. (2016). Are oxygen limitations under recognized regulators of organic carbon turnover in upland soils? *Biogeochemistry*, *127*, 157–171. https://doi.org/10.1007/s10533-015-0180-6

Keiluweit, M., Wanzek, T., Kleber, M., Nico, P., & Fendorf, S. (2017). Anaerobic microsites have an unaccounted role in soil carbon stabilization. *Nature Communications*, 8. https://doi.org/10.1038/s41467-017-01406-6

Krause, H. M., Thonar, C., Eschenbach, W., Well, R., Mäder, P., Behrens, S., … Gattinger, A. (2017). Long term farming systems affect soils potential for N_2O production and reduction processes under denitrifying conditions. *Soil Biology & Biochemistry*, *114*, 31–41. https://doi.org/10.1016/j.soilbio.2017.06.025

Kravchenko, A. N., Negassa, W. C., Guber, A. K., & Rivers, M. L. (2015). Protection of soil carbon within macro-aggregates depends on intra-aggregate pore characteristics. *Scientific Reports*, *5*, 16261. https://doi.org/10.1038/srep16261

Kravchenko, A. N., Negassa, W., Guber, A. K., & Schmidt, S. (2014). New approach to measure soil particulate organic matter in intact samples using X-ray computed microtomography. *Soil Science Society of America Journal*, *78*, 1177–1185. https://doi.org/10.2136/sssaj2014.01.0039

Kravchenko, A. N., Toosi, E. R., Guber, A. K., Ostrom, N. E., Yu, J., Azeem, K., … Robertson, G. P. (2017). Hotspots of soil N_2O emission enhanced through water absorption by plant residue. *Nature Geoscience*, *10*, 496. https://doi.org/10.1038/ngeo2963

Lagomarsino, A., Agnelli, A. E., Pastorelli, R., Pallara, G., Rasse, D. P., & Silvennoinen, H. (2016). Past water management affected GHG production and microbial community pattern in Italian rice paddy soils. *Soil Biology & Biochemistry*, *93*, 17–27. https://doi.org/10.1016/j.soilbio.2015.10.016

Laughlin, R. J., & Stevens, R. J. (2002). Evidence for fungal dominance of denitrification and codenitrification in a grassland soil. *Soil Science Society of America Journal*, *66*, 1540–1548. https://doi.org/10.2136/sssaj2002.1540

Li, X. X., Sorensen, P., Olesen, J. E., & Petersen, S. O. (2016). Evidence for denitrification as main source of N2O emission from residue-amended soil. *Soil Biology & Biochemistry*, *92*, 153–160. https://doi.org/10.1016/j.soilbio.2015.10.008

Loecke, T. D., & Robertson, G. P. (2009). Soil resource heterogeneity in terms of litter aggregation promotes nitrous oxide fluxes and slows decomposition. *Soil Biology & Biochemistry*, *41*, 228–235. https://doi.org/10.1016/j.soilbio.2008.10.017

Mangalassery, S., Sjögersten, S., Sparkes, D. L., Sturrock, C. J., Craigon, J., & Mooney, S. J. (2014). To what extent can zero tillage lead to a reduction in greenhouse gas emissions from temperate soils? *Scientific Reports*, *4*, 4586. https://doi.org/10.1038/srep04586

Mangalassery, S., Sjogersten, S., Sparkes, D. L., Sturrock, C. J., & Mooney, S. J. (2013). The effect of soil aggregate size on pore structure and its consequence on emission of greenhouse gases. *Soil & Tillage Research*, *132*, 39–46. https://doi.org/10.1016/j.still.2013.05.003

Milliken, G. A., & Johnson, D. E. (2001) *Analysis of messy data volume III: Analysis of covariance*. Boca Raton, FL: CRC Press.

Milliken, G. A., & Johnson, D. E. (2009). *Analysis of messy data volume I: Designed experiments*. Boca Raton, FL: CRC Press.

Mooney, S. J., & Morris, C. (2008). Morphological approach to understanding preferential flow using image analysis with dye tracers and X-ray computed tomography. *Catena*, *73*, 204–211.

Mutegi, J. K., Munkholm, L. J., Petersen, B. M., Hansen, E. M., & Petersen, S. O. (2010). Nitrous oxide emissions and controls as influenced by tillage and crop residue management strategy. *Soil Biology & Biochemistry*, *42*, 1701–1711. https://doi.org/10.1016/j.soilbio.2010.06.004

Negassa, W., Guber, A. K., Kravchenko, A. N., Marsh, T. L., Hildebrandt, B., & Rivers, M. L. (2015). Properties of soil pore space regulate pathways of plant residue decomposition and community structure of associated bacteria. *PLOS ONE*, *10*(4), e0123999. https://doi.org/10.1371/journal.pone.0123999.

Nunan, N., Wu, K. J., Young, I. M., Crawford, J. W., & Ritz, K. (2003). Spatial distribution of bacterial communities and their relationships with the micro-architecture of soil. *FEMS Microbiology Ecology*, *44*, 203–215. https://doi.org/10.1016/S0168-6496(03)00027-8

Oates, L. G., Duncan, D. S., Gelfand, I., Millar, N., Robertson, G. P., & Jackson, R. D. (2016). Nitrous oxide emissions during establishment of eight alternative cellulosic bioenergy cropping systems in the North Central United States. *Global Change Biology Bioenergy*, *8*, 539–549. https://doi.org/10.1111/gcbb.12268

Opdyke, M. R., Ostrom, N. E., & Ostrom, P. H. (2009). Evidence for the predominance of denitrification as a source of N2O in temperate agricultural soils based on isotopologue measurements. *Global Biogeochemical*, *Cycles*, 23.

Ostrom, N. E., Gandhi, H., Coplen, T. B., Toyoda, S., Böhlke, J. K., Brand, W. A., … Well, R. (2018). Preliminary assessment of stable nitrogen and oxygen isotopic composition of USGS51 and USGS52 nitrous oxide reference gases and perspectives on calibration needs. *Rapid Communications in Mass Spectrometry*, *32* (15), 1207–1214. https://doi.org/10.1002/rcm.8157

Ostrom, N. E., & Ostrom, P. H. (2011). The Isotopomers of nitrous oxide: Analytical considerations and application to resolution of microbial production pathways. *Handbook of Environmental Isotope Geochemistry*, *1,2*, 453–476.

Ostrom, N. E., Pitt, A., Sutka, R., Ostrom, P. H., Grandy, A. S., Huizinga, K. M., & Robertson, G. P. (2007). Isotopologue effects during N2O reduction in soils and in pure cultures of denitrifiers. *Journal of Geophysical Research-Biogeosciences*, 112. https://doi.org/10.1029/2006JG000287

Ostrom, N. E., Sutka, R., Ostrom, P. H., Grandy, A. S., Huizinga, K. M., Gandhi, H., … Robertson, G. P. (2010). Isotopologue data reveal bacterial denitrification as the primary source of N_2O during a high flux event following cultivation of a native temperate grassland. *Soil Biology & Biochemistry*, *42*, 499–506. https://doi.org/10.1016/j.soilbio.2009.12.003

Parkin, T. B. (1987). Soil microsites as a source of denitrification variability. *Soil Science Society of America Journal*, *51*, 1194–1199.

Paustian, K., Lehmann, J., Ogle, S., Reay, D., Robertson, G. P., & Smith, P. (2016). Climate-smart soils. *Nature*, *532*, 49–57. https://doi.org/10.1038/nature17174

Porre, R. J., Van Groenigen, J. W., De Deyn, G. B., De Goede, R. G. M., & Lubbers, I. M. (2016). Exploring the relationship between soil mesofauna, soil structure and N_2O emissions. *Soil Biology & Biochemistry*, *96*, 55–64. https://doi.org/10.1016/j.soilbio.2016.01.018

Prendergast-Miller, M. T., Baggs, E. M., & Johnson, D. (2011). Nitrous oxide production by the ectomycorrhizal fungi *Paxillus involutus* and *Tylospora fibrillosa*. *Fems Microbiology Letters*, *316*, 31–35. https://doi.org/10.1111/j.1574-6968.2010.02187.x

Qin, Z. C., Zhuang, Q. L., & Zhu, X. D. (2015). Carbon and nitrogen dynamics in bioenergy ecosystems: 2. Potential greenhouse gas emissions and global warming intensity in the conterminous United States. *Global Change Biology Bioenergy*, *7*, 25–39. https://doi.org/10.1111/gcbb.12106

Quigley, M., Rivers, M. L., & Kravchenko, A. N. (2018). Patterns and sources of spatial heterogeneity in soil matrix from contrasting long term management practices. *Frontiers in Environmental Science, for Special Topic Elucidating Microbial Processes in Soils and Sediments: Microscale Measurements and Modeling*, *6*, Article 28. https://doi.org/10.3389/fenvs.2018.00028.

Rabot, E., Henault, C., & Cousin, I. (2014). Temporal variability of nitrous oxide emissions by soils as affected by hydric history. *Soil Science Society of America Journal*, *78*, 434–444. https://doi.org/10.2136/sssaj2013.07.0311

Rabot, E., Henault, C., & Cousin, I. (2016). Effect of the soil water dynamics on nitrous oxide emissions. *Geoderma*, *280*, 38–46. https://doi.org/10.1016/j.geoderma.2016.06.012

Rabot, E., Lacoste, M., Henault, C., & Cousin, I. (2015) Using X-ray computed tomography to describe the dynamics of nitrous oxide

emissions during soil drying. *Vadose Zone Journal*, *14*. https://doi.org/10.2136/vzj2014.12.0177

Robertson, G. P., & Hamilton, S. K. (2015) Long-term ecological research in agricultural landscapes at the Kellogg Biological Station LTER site: conceptual and experimental framework. In: S. K. Hamilton, J. E. Doll, & G. P. Robertson (eds) *The ecology of agricultural landscapes: long-term research on the path to sustainability*. New York, NY: Oxford University Press.

Robertson, G. P., Paul, E. A., & Harwood, R. R. (2000). Greenhouse gases in intensive agriculture: Contributions of individual gases to the radiative forcing of the atmosphere. *Science*, *289*, 1922–1925. https://doi.org/10.1126/science.289.5486.1922

Robertson, G. P., & Tiedje, J. M. (1987). Nitrous-oxide sources in aerobic soils - nitrification, denitrification and other biological processes. *Soil Biology & Biochemistry*, *19*, 187–193. https://doi.org/10.1016/0038-0717(87)90080-0

Rohe, L., Anderson, T. H., Braker, G., Flessa, H., Giesemann, A., Lewicka-Szczebak, D., … Well, R. (2014). Dual isotope and isotopomer signatures of nitrous oxide from fungal denitrification - a pure culture study. *Rapid Communications in Mass Spectrometry*, *28*, 1893–1903. https://doi.org/10.1002/rcm.6975

Sanford, G. R., Oates, L. G., Jasrotia, P., Thelen, K. D., Robertson, G. P., & Jackson, R. D. (2016). Comparative productivity of alternative cellulosic bioenergy cropping systems in the North Central USA. *Agriculture Ecosystems & Environment*, *216*, 344–355.

Schindelin, J., Arganda-Carreras, I., Frise, E., Kaynig, V., Longair, M., Pietzsch, T., … Tinevez, J. Y. (2012). Fiji: An open-source platform for biological-image analysis. *Nature Methods*, *9*, 676–682. https://doi.org/10.1038/nmeth.2019

Schurgers, G., Dorsch, P., Bakken, L., Leffelaar, P., & Haugen, L. E. (2006). Modelling soil anaerobiosis from water retention characteristics and soil respiration. *Soil Biology & Biochemistry*, *38*, 2637–2644. https://doi.org/10.1016/j.soilbio.2006.04.016

Sexstone, A. J., Revsbech, N. P., Parkin, T. B., & Tiedje, J. M. (1985). Direct measurement of oxygen profiles and denitrification rates in soil aggregates. *Soil Science Society of America Journal*, *49*, 645–651.

Smith, K. A. (2017). Changing views of nitrous oxide emissions from agricultural soil: Key controlling processes and assessment at different spatial scales. *European Journal of Soil Science*, *68*, 137–155. https://doi.org/10.1111/ejss.12409

Sprunger, C. D., Oates, L. G., Jackson, R. D., & Robertson, G. P. (2017). Plant community composition influences fine root production and biomass allocation in perennial bioenergy cropping systems of the upper Midwest, USA. *Biomass & Bioenergy*, *105*, 248–258.

Sprunger, C. D., & Robertson, G. P. (2018). Early accumulation of active fraction soil carbon in newly established cellulosic biofuel systems. *Geoderma*, *318*, 42–51. https://doi.org/10.1016/j.geoderma.2017.11.040

Sutka, R. L., Adams, G. C., Ostrom, N. E., & Ostrom, P. H. (2008). Isotopologue fractionation during N_2O production by fungal denitrification. *Rapid Communications in Mass Spectrometry*, *22*, 3989–3996.

Sutka, R. L., Ostrom, N. E., Ostrom, P. H., Breznak, J. A., Gandhi, H., Pitt, A. J., & Li, F. (2006). Distinguishing nitrous oxide production from nitrification and denitrification on the basis of isotopomer abundances. *Applied and Environmental Microbiology*, *72*, 638–644. https://doi.org/10.1128/AEM.72.1.638-644.2006

Sutka, R. L., Ostrom, N. E., Ostrom, P. H., Gandhi, H., & Breznak, J. A. (2004). Nitrogen isotopomer site preference of N_2O produced by *Nitrosomonas europaea* and *Methylococcus capsulatus* Bath (vol 18, pg 1411, 2004). *Rapid Communications in Mass Spectrometry*, *18*, 1411–1412. https://doi.org/10.1002/rcm.1482

Tiedje, J. M., Sexstone, A. J., Parkin, T. B., Revsbech, N. P., & Shelton, D. R. (1984). Anaerobic processes in soil. *Plant and Soil*, *76*, 197–212. https://doi.org/10.1007/BF02205580

Toyoda, S., & Yoshida, N. (1999). Determination of nitrogen isotopomers of nitrous oxide on a modified isotope ratio mass spectrometer. *Analytical Chemistry*, *71*, 4711–4718. https://doi.org/10.1021/ac9904563

Van Groenigen, K. J., Osenberg, C. W., & Hungate, B. A. (2011). Increased soil emissions of potent greenhouse gases under increased atmospheric CO_2. *Nature*, *475*, 214–U121. https://doi.org/10.1038/nature10176

Vogel, H. J., Weller, U., & Schluter, S. (2010). Quantification of soil structure based on Minkowski functions. *Computers & Geosciences*, *36*, 1236–1245. https://doi.org/10.1016/j.cageo.2010.03.007

Walter, K., Don, A., & Flessa, H. (2015). Net N_2O and CH_4 soil fluxes of annual and perennial bioenergy crops in two central German regions. *Biomass & Bioenergy*, *81*, 556–567. https://doi.org/10.1016/j.biombioe.2015.08.011

Wang, W., Kravchenko, A. N., Smucker, A. J. M., Liang, W., & Rivers, M. L. (2012). Intra-aggregate pore characteristics: X-ray computed microtomography analysis. *Soil Science Society of America Journal*, *76*, 1159–1171. https://doi.org/10.2136/sssaj2011.0281

Well, R., Kurganova, I., De Gerenyu, V. L., & Flessa, H. (2006). Isotopomer signatures of soil-emitted N_2O under different moisture conditions - A microcosm study with arable loess soil. *Soil Biology & Biochemistry*, *38*, 2923–2933. https://doi.org/10.1016/j.soilbio.2006.05.003

Wightman, J. L., Duxbury, J. M., & Woodbury, P. B. (2015). Land quality and management practices strongly affect greenhouse gas emissions of bioenergy feedstocks. *Bioenergy Research*, *8*, 1681–1690. https://doi.org/10.1007/s12155-015-9620-3

Wuensch, K. L. (2016). An introduction to path analysis. Retrieved from https://core.ecu.edu/psyc/wuenschk/MV/SEM/Path.pdf on 07/10/2018

Zhu-Barker, X., Cavazos, A. R., Ostrom, N. E., Horwath, W. R., & Glass, J. B. (2015). The importance of abiotic reactions for nitrous oxide production. *Biogeochemistry*, *126*, 251–267. https://doi.org/10.1007/s10533-015-0166-4

SUPPORTING INFORMATION

Additional supporting information may be found online in the Supporting Information section at the end of the article.

How to cite this article: Kravchenko AN, Guber AK, Quigley MY, Koestel J, Gandhi H, Ostrom NE. X-ray computed tomography to predict soil N_2O production via bacterial denitrification and N_2O emission in contrasting bioenergy cropping systems. *GCB Bioenergy*. 2018;00:1–17. https://doi.org/10.1111/gcbb.12552